Stabilization of Hypersonic Boundary Layer by 2-D Surface Roughness

Kahei Danny Fong[1], Xiaowen Wang[2] and Xiaolin, Zhong[3]
University of California Los Angeles, Los Angeles, CA, 90095

It has been shown previously the relative location of 2D roughness element and the synchronization point is important in determining roughness effect on modal growth. In particular, it is found if roughness is placed at or downstream of synchronization point, perturbation can be damped by roughness. In this paper, the results of further parametric studies are presented. In addition, mean flows with and without roughness are examined by numerical simulation and linear stability theory (LST) to understand the mechanism of damping and amplifying effects on perturbation. It is found that roughness alters mean flow profiles which can possibly contribute to destabilization of first mode and stabilization of second mode. It is also found that LST is capable of predicting such stabilizing and destabilizing effects. Furthermore, numerical study on a supersonic Mach 3 flow in which only first mode exists is conducted. The results show roughness in this flow amplifies perturbation at all frequencies which confirms our hypothesis about the importance of synchronization location and roughness. The results can potentially lead to a new passive flow control method.

I. Introduction

ROUGHNESS induced transition has a great impact on the development of hypersonic vehicles[1]. For example, transition can have a first-order impact on the lift and drag, stability and control, and heat transfer properties of the vehicles [2]. Roughness induced transition is an important consideration in the design of thermal protection systems (TPS) of hypersonic vehicles [3, 4]. For a reentry vehicle entering earth's atmosphere, it initially experiences a heating environment associated with a laminar boundary layer. As the vehicle altitude decreases, the vehicle surface becomes rougher and the boundary layer becomes turbulent. The transition from a laminar boundary layer to a turbulent one leads to the increase of surface heating rates by a factor of five or more. Thus, the ability to understand the physics of roughness induced transition plays an essential role in the design of TPS for reentry vehicles. Currently, roughness induced laminar-turbulent transition in hypersonic boundary layers, especially that induced by arbitrary surface roughness, is still poorly understood due to the limitation in experimental facilities and numerical methods [5].

Ideally the laminar-turbulent transition process can be divided into four stages. The first stage involves small disturbance fields which are initialized via a process termed "receptivity" by the viscous flow. The initial disturbance fields can involve both free stream and vehicle self-induced fluctuations such as acoustics, dynamic vortices, entropy spottiness, etc. The next stage is the linear growth stage, where small disturbances are amplified until they reach certain amplitude where nonlinear effects become important. The amplification can be in the form of exponential growth of Eigen modes (Tollmien-Schlichting waves or Mack waves) and non-modal growth of optimal disturbances (Transient growth). Once a disturbance has reached finite amplitude, it often saturates and transforms the flow into a new, possibly unsteady state, which is termed as the secondary instability stage. The last stage is the breakdown stage where nonlinearities and/or high-order instabilities excite an increasing number of scales and frequencies in the flow.

[1] Graduate Student Researcher, Mechanical and Aerospace Engineering Department, 48-121 Engineering IV, 420 Westwood Plaza, Los Angeles, CA 90095-1597, AIAA student member
[2] Research Associate, Mechanical and Aerospace Engineering Department, 48-121 Engineering IV, 420 Westwood Plaza, Los Angeles, CA 90095-1597, AIAA member
[3] Professor, Mechanical and Aerospace Engineering Department, 48-121 Engineering IV, 420 Westwood Plaza, Los Angeles, CA 90095-1597, AIAA associate fellow

The receptivity study is mainly concerned with the excitation of instability waves, the characteristics of which can be analyzed by the linear stability theory (LST) [6]. The LST analyzes the propagation of individual sinusoidal waves in the streamwise direction inside the boundary layer. These waves are referred as Tollmien-Schlichting (T-S) waves for low speed flow, whose amplitudes vary though the boundary layer and die off exponentially outside the boundary layer. Extensive numerical and theoretical researches have been conducted to solve the linearized Navier-Stokes equations and many characteristics regarding the instability waves in hypersonic boundary layers have been discovered [6-10]. Mack [6] identified the unstable modes by using the LST for compressible flow. He showed that inside a supersonic boundary layer, there are multiple higher instability modes in addition to the first mode, which is the compressible counterpart of T-S waves in the incompressible boundary layers. These instability modes in the supersonic boundary layer are termed as first mode, second mode, third mode, etc. For supersonic boundary layer with Mach number larger than four, Mack's second mode is the most unstable mode, and it plays an important role in hypersonic boundary layer transition.

Direct numerical simulation has become an effective research tool for studying hypersonic boundary layer receptivity, stability, and transition by numerically solving the time-dependent three-dimensional Navier–Stokes equations for the temporally or spatially evolving instability waves. Malik et al. [11] investigated the responses of a Mach 8 flow over a sharp wedge of a half-angle of 5.3^{o} to three types of external forcing: a planar freestream acoustic wave, a narrow acoustic beam enforced on the bow shock near the leading edge, and a blowing-suction slot on the wedge surface. They concluded that these three types of forcing eventually resulted in the same type of instability waves in the boundary layer. Ma and Zhong[12] studied the receptivity mechanisms of the same hypersonic boundary layer to various freestream disturbances, i.e., fast and slow acoustic waves, vorticity waves, and entropy waves, by solving the two-dimensional compressible Navier-Stokes equations. They found that the stable modes in the boundary layer played a very important role in the receptivity process. Recently, Wang et al. [13] further studied the response of the Mach 8 flow over a 5.3^{o} half-angle sharp wedge to wall blowing–suction. The results showed that mode S is strongly excited when the actuator is located upstream of the corresponding synchronization point. There is no significant amplification of pressure perturbation when the actuator is downstream of the synchronization point. Although the exact cause and mechanism of this result were not clear, such a result was obtained for wall blowing–suction at all frequencies considered in their study. Balakumar[14] numerically investigated the receptivity of a 2-D roughness to acoustic waves and found the isolated roughness does not contribute much in generating unstable disturbances. Marxen et al. [15] simulated the effects of a localized two-dimensional roughness element on the disturbance amplification in a hypersonic boundary layer. Their numerical experiments showed that in the vicinity of the separation regions, which are located in the upstream and downstream of the roughness, an increased amplification of a second-mode disturbance occurs for a certain frequency.

Roughness has long been used to trip boundary layer to turbulence, but studies have been found that roughness is capable of stabilizing boundary layer as well. Back in 1959, James [16] studied the effect of Mach number and surface roughness on a hollow cylinder. He found that there existed an optimum roughness height which gave a maximum laminar run than a small surface. It implied that roughness can possibly delay transition. In 1964, Holloway and Sterrett [17] performed experiments on a boundary layer at Mach 4.0 and 6.0 with surface roughness at different local Reynolds number. They found that under certain circumstances, roughness with height less than boundary layer thickness can delay the transition onset on the flat plate compared with no roughness situation. However, no physical reasons had been given in the paper. Later, Fujii investigated the effect of two dimensional surface roughness on a hypersonic boundary layer[18]. The experiment was carried out at the JAXA 0.5m hypersonic wind tunnel using a 5 deg half angle sharp cone. It was found that wavy wall roughness can delay transition.

In our previous studies [19, 20], a systematic study of the two dimensional roughness effects on modal growth is performed on a hypersonic flat plate at Mach 5.92. The roughness is modeled as a two dimensional bump and is treated by a previously developed high-order cut cell method. Roughness locations and heights have been varied to study their effects respectively. For unsteady simulation, pure mode S and mode F perturbation at $100kHz$ are found by LST analysis and are imposed into the meanflow separately. Our results show that when roughness is located very far upstream of the synchronization point of the imposed frequency, the roughness effect is weak. However, when roughness is placed a little bit downstream but still upstream of the synchronization point, perturbation is amplified. The strength of amplification is related to the roughness height. In our test cases, a tall roughness (but still within the local boundary layer thickness) always results a stronger amplification. As roughness moves downstream to a location which is exactly the synchronization point location, it is found that the perturbation is damped. Moving roughness to a location more downstream of synchronization point makes the damping effect more profound. Similar to the amplification result, roughness height controls the damping in this location as well. Tall roughness results a stronger damping on the perturbation. Moreover, a wall normal velocity pulse which has a frequency

bandwidth of 1MHz confirms our mode S/F results on the importance of synchronization point and roughness location. It is found that roughness at a fixed location is capable of damping perturbations around frequencies close to the synchronization point frequency which corresponds to the roughness location.

In this paper, the systematic investigation is extended to study the effects of roughness width and multiple roughness elements. Moreover, mean flows with and without roughness are examined by numerical simulation and linear stability theory to understand the mechanism of damping and amplifying effects on perturbation. It is found that roughness alters mean flow profiles such that first mode is stabilized while the alteration destabilizes second mode. To further validate the results, a 'slow' supersonic flow simulation (Mach 3) in which only first mode exists is studied. Our results show that roughness in this slow flow amplifies first mode perturbation at all frequencies which confirms our hypothesis that roughness effects on hypersonic boundary-layer stabilities are caused by the alteration of mean flow. Our results can possibly lead to a new passive flow control method and to explain roughness delay transition in some experiments.

II. Governing Equations

For direct numerical simulation of hypersonic boundary layer transition, the governing equations are the three-dimensional Navier–Stokes equations. We assume that we are dealing with Newtonian fluids with the perfect gas assumption and isothermal wall conditions. The governing equations can be written in the following conservation-law form in the Cartesian coordinates,

$$\frac{\partial U}{\partial t}+\frac{\partial F_j}{\partial x_j}+\frac{\partial F_{vj}}{\partial x_j}=0 \tag{1}$$

where U, F_j and F_{vj} are the vectors of flow variables, convective flux, and viscous flux in the *jth* spatial direction respectively, i.e.,

$$U=\left\{\rho,\rho u_1,\rho u_2,\rho u_3,e\right\} \tag{2}$$

$$F_j=\begin{Bmatrix}\rho u_j\\ \rho u_1u_j+p\delta_{1j}\\ \rho u_2u_j+p\delta_{1j}\\ \rho u_3u_j+p\delta_{1j}\\ (e+p)u_j\end{Bmatrix} \tag{3}$$

$$F_{vj}=\begin{Bmatrix}0\\ \tau_{1j}\\ \tau_{2j}\\ \tau_{3j}\\ \tau_{jk}u_k-q_j\end{Bmatrix} \tag{4}$$

In this paper, only perfect-gas hypersonic flow is considered, i.e.,

$$p=\rho RT \tag{5}$$

$$e=\rho(C_vT+\frac{1}{2}u_ku_k) \tag{6}$$

$$\tau_{ij} = \mu(\frac{\partial u_i}{\partial x_j} + \frac{\partial u_j}{\partial x_i}) + \delta_{ij}\lambda\frac{\partial u_k}{\partial x_k} \tag{7}$$

$$q_j = -k\frac{\partial T}{\partial x_j} \tag{8}$$

where R is the gas constant. The specific heat C_v is assumed to be constant with a given ratio of specific heats γ. The viscosity coefficient μ can be calculated by Sutherland's law in the form:

$$\mu = \mu_r\left(\frac{T}{T_0}\right)^{3/2}\frac{T_0 + T_s}{T + T_s} \tag{9}$$

where, for air, $\mu_r = 1.7894\times10^{-5}\,Ns/m^2, T_0 = 288.0K, T_s = 110.33K$ and λ is assumed to be $-2/3\mu$. The heat conductivity coefficient k can be computed through a constant Prantl number.

III. High Order Cut-Cell Method

A schematic of a computational domain and a cut-cell grid in roughness induced hypersonic boundary layer transition is shown in Figure 1. This figure shows a typical hypersonic flow over a blunt body, where a bow shock is created by the supersonic freestream. In this paper, a high-order shock-fitting method is used to track the movement of the bow shock which is treated as the upper boundary of the computational domain. The computational grid for a shock-fitting formulation is bounded between the bow shock above and the blunt body below. The cut-cell grid is a smooth curvilinear grid fitted to the baseline body shape without the roughness. As a result, the roughness surface cuts across the grid lines. The roughness surface, Γ, is represented by surface equation in the following form,

$$\Gamma: f(x, y, z) = 0 \tag{10}$$

For a problem concerning practical arbitrary roughness, it is likely that there is no analytical equation applicable to represent the shape of the roughness element. In this case, of n discrete points $\{(x_1, y_1, z_1), (x_2, y_2, z_2), \ldots, (x_n, y_n, z_n)\}$ are used to represent the surface.

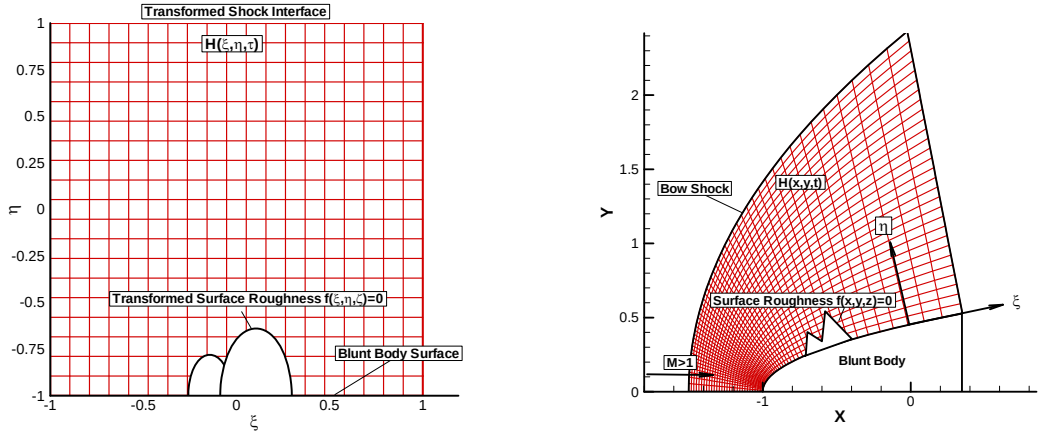

(a) **(b)**

Figure 1.Physical and computational domain and a cut-cell grid of hypersonic flow over a blunt body with surface roughness: a) physical grid, b) computational grid with a transformed roughness

Both the governing Eq. (1) and the roughness equation (10) in the physical domain are transformed into a Cartesian computational domain bounded by bow shock and flat plate. Under the computational coordinate system, the body fitted grids are represented by a curvilinear three-dimensional coordinates (ξ,η,ς) along the grid lines. The unsteady movement of the bow shock is treated as the computational upper boundary located at $\eta=\eta_{\max}$, which is time dependent. The other grid lines $\xi=const$ and $\varsigma=const$ remains stationary during computations. The coordinate transformation is defined by:

$$\begin{cases}\xi=\xi(x,y,z)\\ \eta=\eta(x,y,z,t)\\ \varsigma=\varsigma(x,y,z)\\ \tau=t\end{cases}\leftrightarrow\begin{cases}x=x(\xi,\eta,\varsigma,\tau)\\ y=y(\xi,\eta,\varsigma,\tau)\\ z=z(\xi,\eta,\varsigma,\tau)\\ t=\tau\end{cases} \tag{11}$$

where (x,y,z,t) are the physical coordinates defined under Cartesian coordinate system.

A third-order accurate Cut-Cell method is used in current numerical simulation [21]. A set of uniformly distributed Cartesian grids can be generated in the computational domain where the grid distribution in the physical domain is not uniformly distributed. Because smooth body-fitted grids are generated in the regular computational domain without the roughness, some of the Cartesian grid cells may be cut by the roughness boundary, which leads to irregular Cartesian grid cells. More details of the grid structure are discussed in a previous paper [21].

IV. Results and Discussion

A. Flow conditions and roughness model

In order to study the roughness effect on modal growth, a meanflow with a finite height surface roughness needs to be simulated. Therefore, the high order cut cell method is used to model an isolated roughness on the surface of a hypersonic flat plate. Both steady and unsteady flows with surface roughness are considered. The freestream condition is the same as those used in used in Maslov's experiment [7] and in our previous studies as follows,

$$\begin{cases}P_r=0.72, R_\infty=\rho_\infty * u_\infty/\mu_\infty=13.2\times10^6/m\\ M_\infty=5.92, T_\infty=48.69K, P_\infty=742.76Pa\end{cases} \tag{12}$$

Where M_∞, T_∞, P_∞, P_r, R_∞ are Mach number, temperature, pressure, Prandtl number and unit Reynolds number, respectively. The flat plate is assumed to be isothermal.

An isolated roughness element of smooth shape is placed on the surface of the flat plate. Motivated by Whiteheard's experiments [22], the shape of the surface roughness is chosen to be a two-dimensional bump, governed by the following elliptic equation,

$$\frac{(x-x_c)^2}{a^2}+\frac{y^2}{b^2}=h^2 \tag{13}$$

where the parameters a, b and h control roughness width and height. In addition, x_c defines the location of the roughness center. The grid size is 241 points in streamwise direction and 121 points in wall-normal direction in each computational zone.

A third-order cut-cell method is used to compute the two-dimensional viscous hypersonic flow over the flat plate with the roughness element. As described, a coordinate transformation is employed to transform the physical domain shown in Figure 1 into a rectangle computational domain with a set of Cartesian grid. The optimal transformation formula is determined by the specific physical problem considered.

B. The effect of roughness and width on perturbation with a wide frequency spectrum

After the steady meanflow with surface roughness is obtained, the pulse model that is implemented in Fong et al [20] is used to disturb the meanflow for unsteady simulations. A hole is modeled on the flat plate located at $x = 0.1m$ with a width of $0.003m$. The hole introduces wall normal velocity perturbation in the flow. At each grid point, the perturbation is Gaussian in time, as shown in Figure 2(a). However, in order not to introduce any additional mass into the meanflow, the perturbation is sinusoidal in space as shown in Figure 2(b). Figure 2(c) shows the FFT spectrum of the perturbation. It can be seen that the pulse has a frequency range around $1MHz$, which is broad enough to cover the most unstable modes in the flow.

This pulse model is implemented into the meanflow in which roughness locates at $x = 0.185m$. Figure 3 shows the pressure perturbation contour resulted from the pulse for roughness with a height of 50% local boundary layer thickness and two local boundary layer thickness width. Both the hole and roughness are also shown. Figure 4 and Figure 5 shows the frequency spectra of the pulse perturbation upstream and downstream of roughness respectively as shown in Fong et al [20]. The roughness location in this case corresponds to the synchronization location for frequency $133.26kHz$ which is highlighted in the figures. The detail of finding synchronization location can be found in Wang et al [23]. It can be seen that for a fixed roughness width, roughness is capable of damping perturbations around frequencies higher than the synchronization frequency both upstream and downstream of roughness compared with no roughness situation. On the other hand, roughness element amplifies perturbations at frequencies lower than the synchronization frequencies.

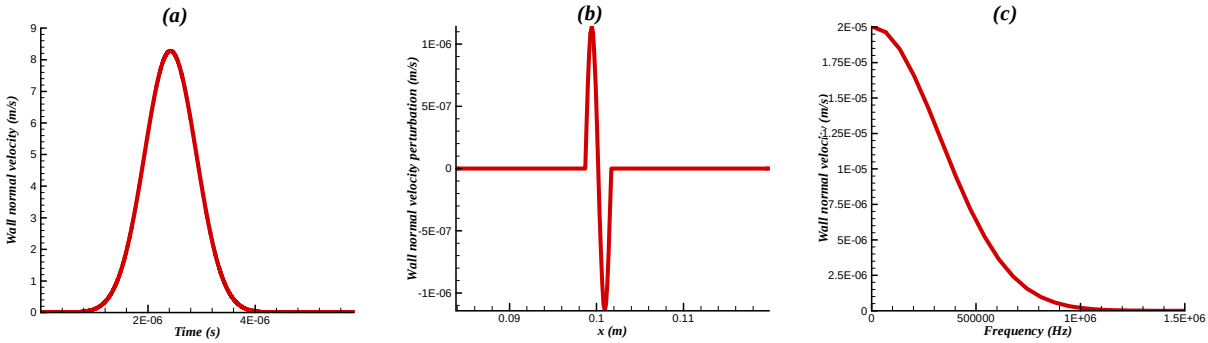

Figure 2.(a) Time history of wall normal velocity on the wall. (b) Snapshot of wall normal velocity in space. (c) FFT result of the Gaussian shape perturbation in (a).

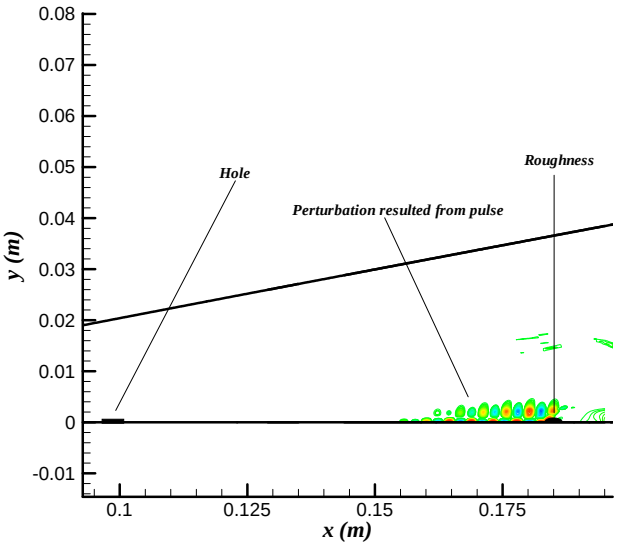

Figure 3.Schematic presentation of numerical setup for the pulse case. The hole to introduce perturbation, roughness and pressure perturbation are shown.

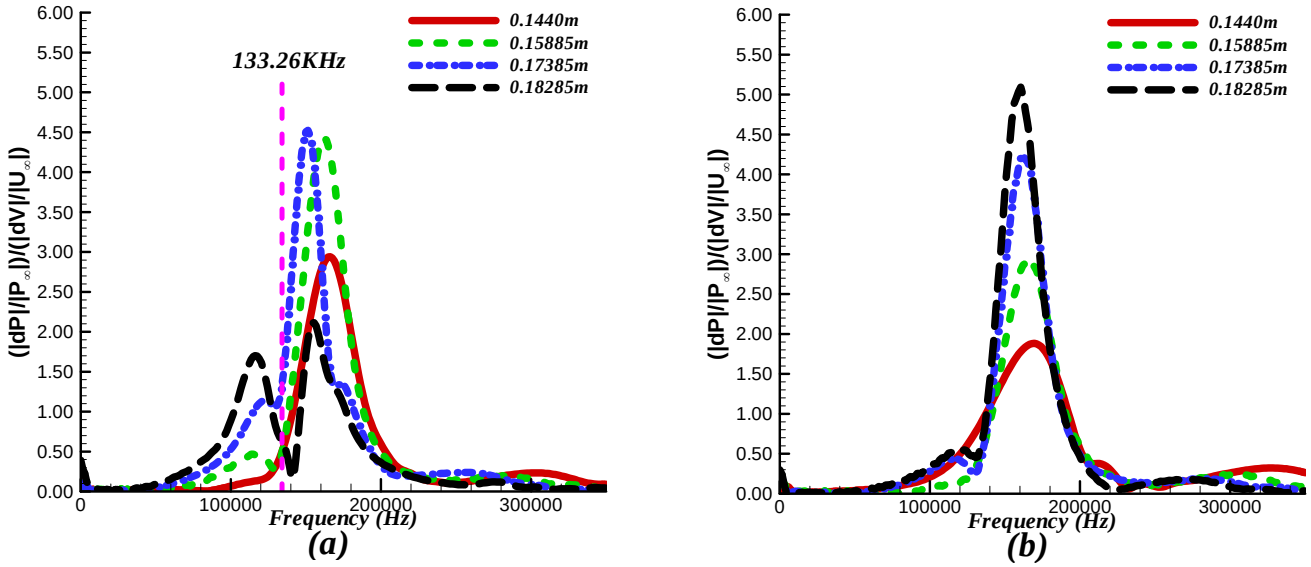

Figure 4. Non-dimensional frequency spectra of wall pressure perturbation at different location. (a) Upstream of roughness (b) No roughness case

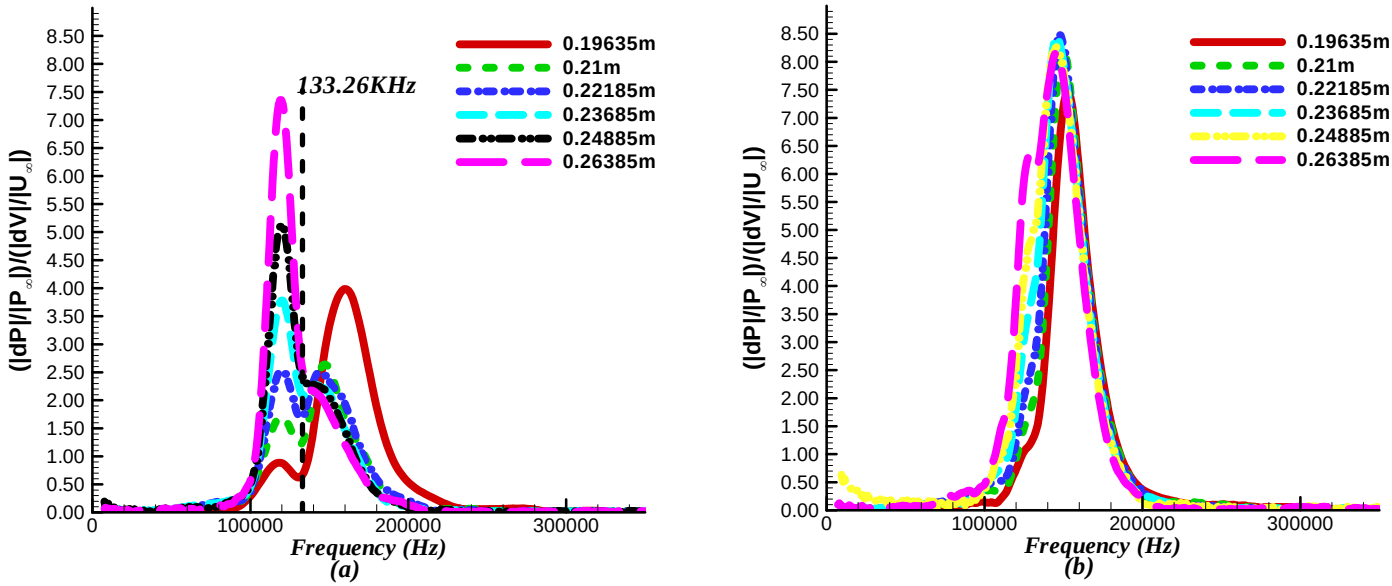

Figure 5. Non-dimensional frequency spectra of wall pressure perturbation at different location. (a) Downstream of roughness (b) No roughness case

It is suspected that roughness width can also alter the effect of roughness on modal growth. In our study, roughness width of 4, 2, 1, 0.5 and 0.25 of local boundary layer thickness are also considered. Figure 6(a) and (b) show the frequency spectrum at location 3.4mm upstream of the leading edge of roughness and 3.4mm downstream of the trailing edge of roughness respectively. It is clearly shown upstream of roughness; the width of roughness has almost no effect on the frequency spectrum. Downstream of roughness, roughness width still has very small effect on perturbation which has frequency lower than the synchronization frequency. However, a relatively big difference

is observed in frequencies higher than the synchronization frequency. Thin roughness results a stronger damping. This is due to the fact that thin roughness is less smooth, which has a more pronounced effect on the mean flow profile than a smooth wider roughness.

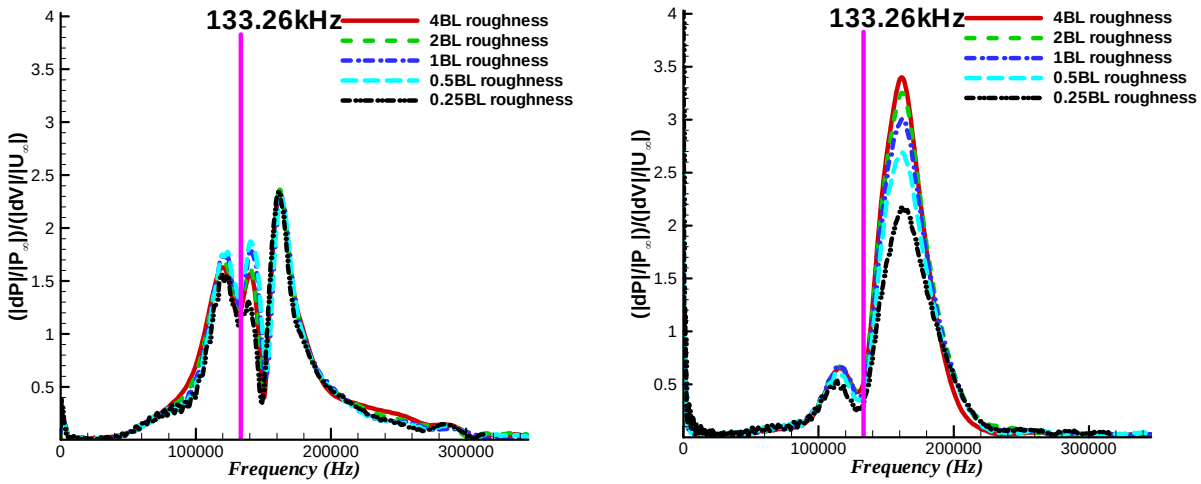

Figure 6. Non-dimensional frequency spectra of wall pressure perturbation for different roughness width (BL in the figure means boundary layer thickness). (a) upstream of roughness (b) downstream of roughness

C. Multiple roughness elements

Hitherto, studies have been focusing on one single roughness element in a hypersonic boundary layer. It is also of interest how multiple roughness elements alter modal growth. Two roughness elements and three roughness elements simulations have also been done. In the two roughness simulation, the first roughness is at, x=0.185m and its height is fixed at 50% local boundary layer thickness while its width is fixed at two local boundary thickness. The second roughness is located in the downstream region of first roughness at x=0.231m, while its height and width are kept the same as the first roughness. The location of first roughness corresponds to the synchronization point of frequency $133.26kHz$, while the location of the second roughness corresponds to the synchronization point of frequency $119.26kHz$.

Figure 7 shows the pressure contour of the two roughness meanflow. It is seen that the second roughness generated the same Mach wave as one roughness case. Moreover, the wave pattern looks very similar to that for the first roughness. In unsteady simulation, the same pulse perturbation is imposed into this meanflow. Therefore, the perturbation would have a frequency range of 1MHz as shown in Figure 2. The pressure perturbation contour is shown in Figure 8. Similar to one roughness case, it is of interest to study how the perturbation interacts with the two roughness elements. Figure 9 shows the spatial development of perturbation at different frequencies. The frequencies chosen are $120kHz$, $130kHz$ and $140kHz$. Since the location of the second roughness corresponds to the synchronization point of frequency $119.26kHz$, it is expected the perturbation at these three frequencies will be damped after the second roughness. Figure 9 confirms the expectation. It is shown that the first roughness amplifies $120kHz$ perturbation since it is upstream of its synchronization point. However, when the perturbation travels downstream and approaches the second roughness, it starts to be damped since the roughness locates very close to its synchronization point. Downstream of the second roughness, the perturbation at $120kHz$ is weaker than the case without roughness. Both roughness damps perturbations at $130kHz$ and $140kHz$ because they are located very close or behind the corresponding synchronization points.

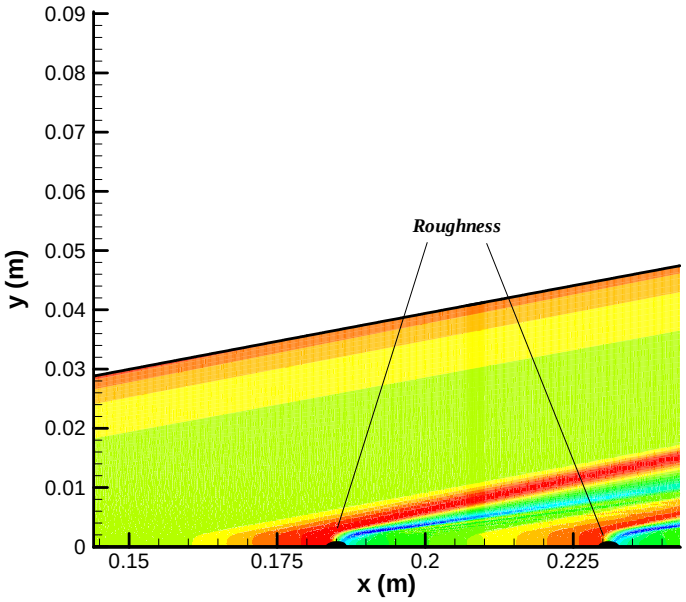

Figure 7. Pressure contour of two roughness meanflow.

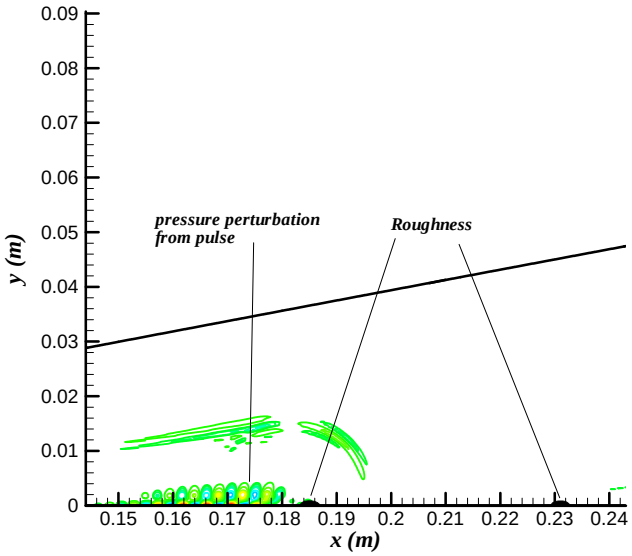

Figure 8. Pressure perturbation contour for two roughness case.

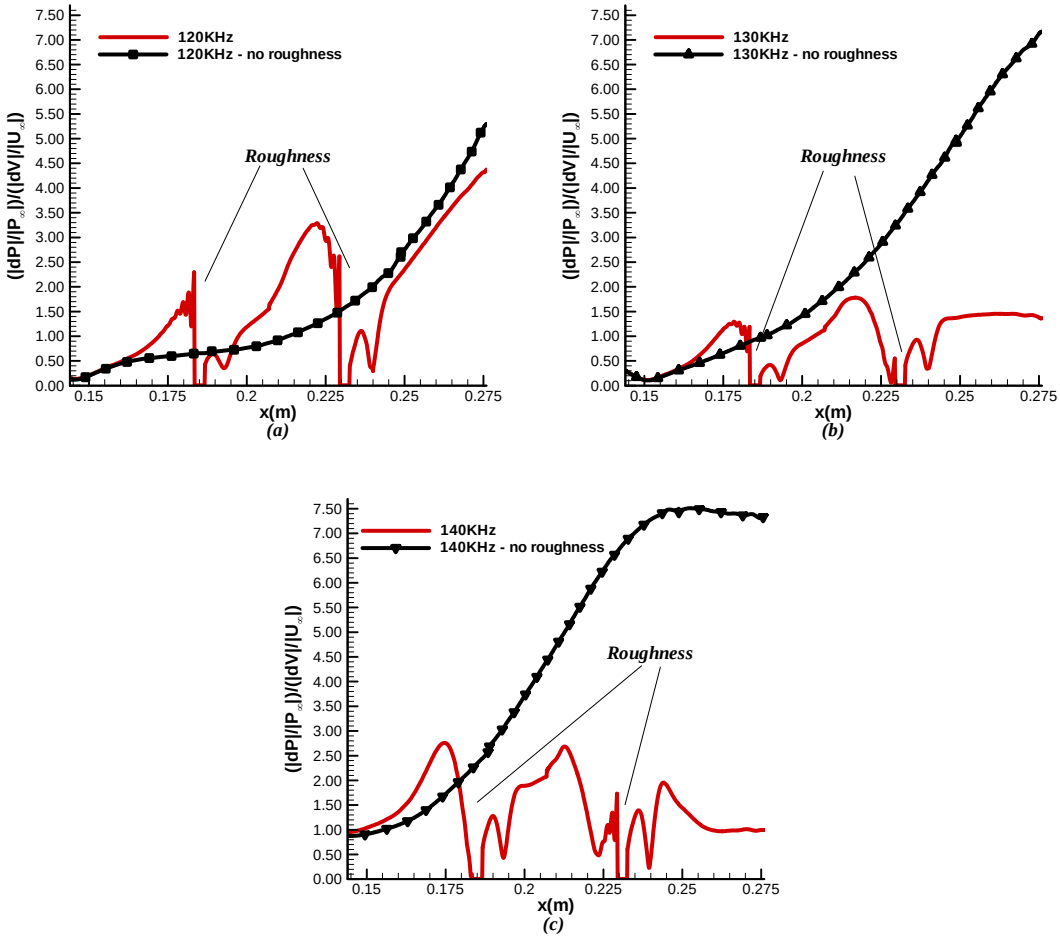

Figure 9. Spatial evolution of wall pressure perturbation for two roughness case at three different frequencies (a) 120 KHz (b) 130 KHz (c) 140 KHz

A three roughness elements simulation has also been conducted. The pressure contour is shown in Figure 10. The wave pattern generated by each roughness is very similar to all previous cases. In this simulation, the first, second and the third roughness element are placed at $x = 0.331m$, $x = 0.3874m$ and $x = 0.4569m$ respectively. These locations correspond to the synchronization location of frequencies: $100kHz$, $92.1kHz$ and $84.7kHz$. The location of roughness in this case is chosen according to the roughness width in the front. For example, the spacing of the second roughness is 10 times the roughness width of the first roughness. On the other hand, the spacing of the third roughness is ten times the roughness width of the second roughness. Since the width and height of each roughness element depends on the local boundary layer thickness, the actual distance between roughness elements is not uniform as shown in Figure 10. The size of roughness used here is 50% local boundary layer thickness height and 2 local boundary layer thickness width. Figure 11 shows the spatial growth of perturbation at $100kHz$. It is clearly seen that this roughness arrangement damps the perturbation very effectively. Without roughness, the perturbation amplitude reaches almost 20 at the end of the figure while with multiple roughness elements, it is only 0.5. The difference is almost 50 times whereas in two roughness arrangement, the difference is only about 8 times. This result suggests that an array of roughness elements can be used to damp disturbance at certain frequency more efficiently.

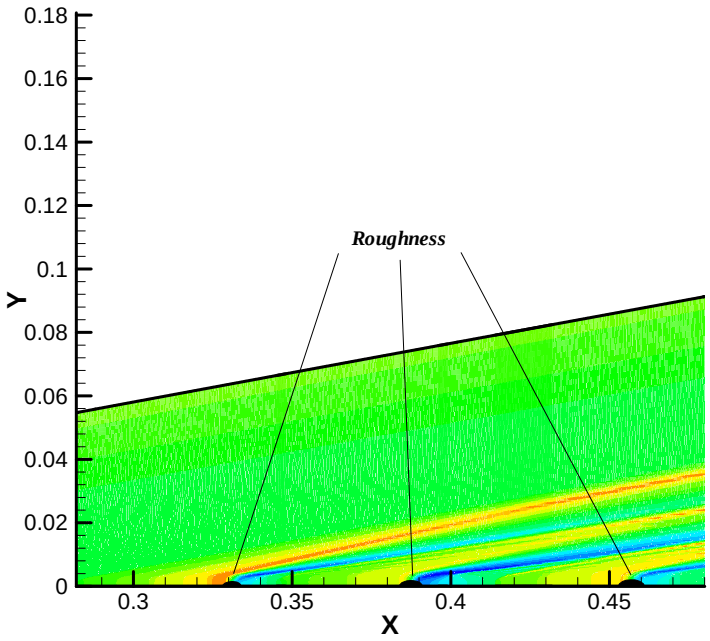

Figure 10. Pressure contour of three roughness meanflow.

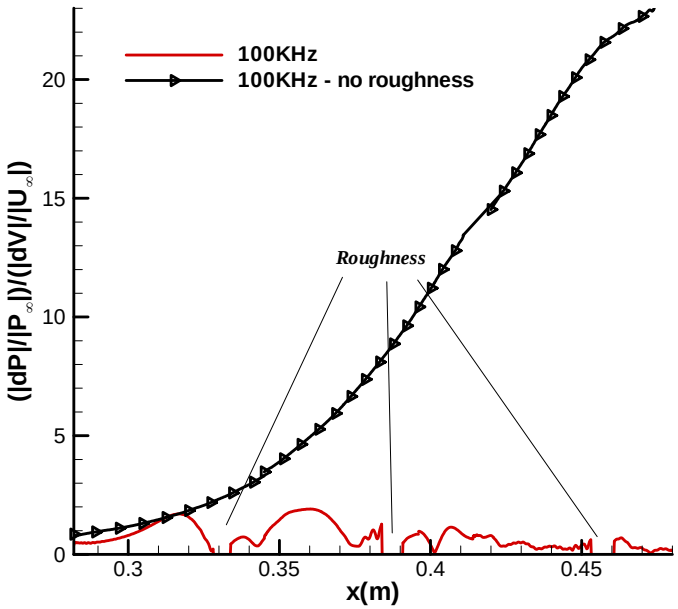

Figure 11.Spatial evolution of wall pressure perturbation for two roughness case at three different frequencies 100KHz

D. Investigation on the Mechanism

All numerical simulations' results have agreed that roughness is able to damp perturbation after its synchronization location. In other word, roughness is capable of damping second mode instability. In order to understand the physical mechanism, the meanflow with and without roughness are examined. Figure 12 shows the schematic of how a roughness element changes the meanflow profile. Typically, a roughness would generate a circulation region in the flow. Thus, the velocity profile around a roughness is not as smooth as that without a roughness element. Figure 13 (a) shows the velocity profile behind a roughness comparing with no roughness situation. It is seen that roughness has increased the boundary layer thickness; it also creates a small circulation in the near wall region and make it less smooth. This change can alter the first mode stability characteristic since it introduces more inflection points in the velocity profile. On the other hand, it is known that the second mode wave belongs to the family of trapped acoustic waves in the region between the wall and the sonic line in perturbation reference frame [24]. In Figure 13 (b), the relative Mach number in perturbation reference frame as defined in Fedorov [24] is shown. The sonic line is also shown. It can be clearly seen that roughness has increase the size of region between the wall the sonic line. The change of such region by roughness is a possible cause of the damping that is observed in numerical simulations.

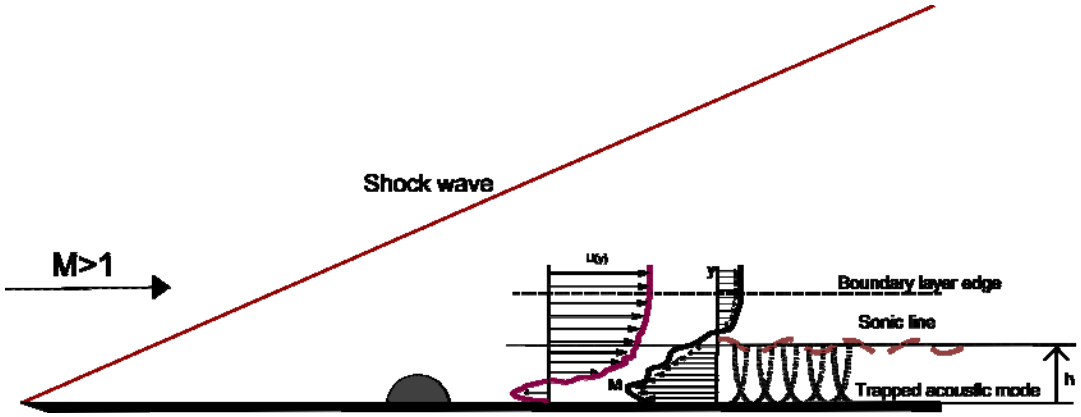

Figure 12. The effect of roughness on the meanflow.

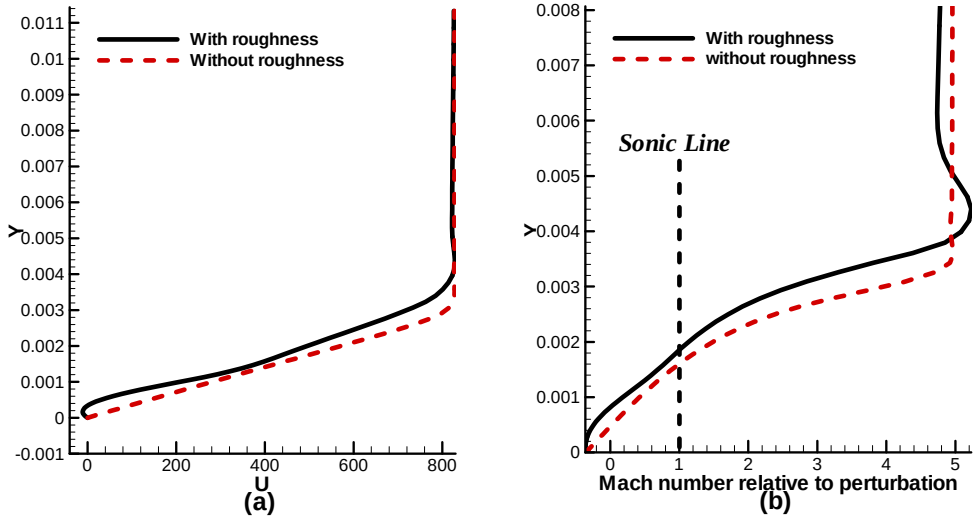

Figure 13. Comparison of meanflow profile with and without roughness (a) velocity profile (b) Sonic line

To further investigate the alteration on meanflow by roughness. Linear stability analysis is used to interpret the results. It is common practice to compare mode shape, wave number and growth rate from LST with direct numerical simulation results. However, wave number and growth rate are non-dimensionalized in our LST. To get dimensional form of growth rate and wave number, the following relation is used as in Ma and Zhong [25],

$$\psi = \frac{\psi'}{\sqrt{\frac{x\mu_\infty}{\rho_\infty U_\infty}}} \tag{14}$$

where ψ and ψ' denote dimensional and non-dimensional parameters respectively. In DNS, the growth rate for a single mode is defined as,

$$\alpha_i = -\frac{1}{\left|H(f_n)\right|}\frac{\mathrm{d}\left|H(f_n)\right|}{\mathrm{d}x} \tag{15}$$

where $H(f_n)$ denotes the amplitude at frequency f_n. Local wave number is defined as,

$$\alpha_r = \frac{\mathrm{d}\varphi_n}{\mathrm{d}x} \tag{16}$$

Where φ_n is the phase angle of $H(f_n)$.

In the LST analysis, roughness is at $x = 0.185m$ in the meanflow. Figure 14 shows the prediction of the wave number and growth rate at frequency range $100kHz$ to $200kHz$ at $x = 0.17385m$, a location upstream of roughness. It is seen that LST suggests the existence of roughness would not change the wave number significantly. The strongest effect on wave number is at around frequency $120kHz$ to $150kHz$ where roughness increases the wave number, or shortens the corresponding wavelength. Although the roughness effect on wave number is weak, LST predicts that its effect on growth rate is very strong as shown in Figure 14 (b). The synchronization frequency for the roughness location, $133.26kHz$, is also shown in this figure. It can be seen the growth rate for perturbation at frequency lower than $130kHz$ is higher than that in no roughness case. The two lines intercepts at frequency around $130kHz$ which is very close to the synchronization frequency. At this point, the growth rate for roughness case and no roughness are the same. After the interception, LST predicts that the growth rate for frequency higher than $130kHz$ is lower in roughness case. In other word, the perturbation at frequency after the synchronization frequency is damped which supports our observation based on DNS results. Figure 15 shows the LST prediction of wave number and growth rate on meanflow with roughness compared with the DNS results at the same location, $x = 0.17385m$. It is seen that LST prediction does not agree very well with DNS. The disagreement can be explained by the violation of parallel flow assumption taken by LST analysis. However, LST analysis is still able to predict the damping effect on growth rate at frequency higher than $130kHz$. DNS result shows that the frequencies between $140kHz$ and $170kHz$ have been damped so much that its growth rate is negative, which means it is stable. LST shows that the frequency in this range is damped but its growth rate is still positive. In other words, LST has underestimated the damping effect by roughness, but it is still able to predict the fundamental effect. The same LST and DNS analysis at a location further downstream of roughness, $x = 0.26385m$, is performed as shown in Figure 16. It is seen that LST prediction on wave number has becomes much more accurate. Moreover, the growth rate predicted by DNS also follows LST prediction in this location. Figure 17 shows the growth rate predicted by LST for meanflow with roughness and without roughness at the same location, DNS results is also included. It is clearly shown the results for no roughness and with roughness case are very similar. The roughness effect in this location is very small.

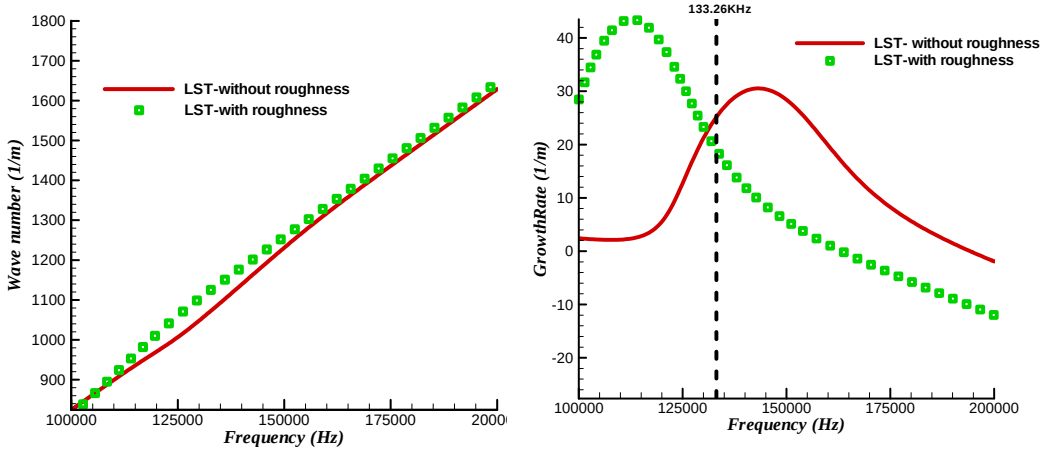

(a) **(b)**

Figure 14. LST prediction of wave number and growth rate for meanflow with roughness and without roughness at $x = 0.17385m$.

Figure 18 shows the pressure perturbation at $118.9kHz$ mode shape comparison between LST and DNS at $x = 0.26385m$,a location far downstream of roughness. The perturbation frequency, $118.9kHz$, is chosen according to the most unstable frequency at this location (the peak as in Figure 5). It shows that the two results agree extremely well within the boundary layer. The small disagreement outside of boundary layer can be explained by the Mach wave generated by surface roughness. Base on the good agreement at this far downstream location behind roughness, it is concluded that non-parallel effect is very strong around the roughness vicinity but gets weaker in downstream direction. Nevertheless, LST would still be able to predict the roughness effect that is observed in numerical simulations. Away from roughness, the comparison between numerical simulation and LST becomes much better.

Based on the results by LST and by investigating the meanflow profile, it can be said that the alteration on the meanflow by roughness can change the stability characteristic. Specifically, the introduction of roughness makes the meanflow less smooth, thus introducing more inflection points. On the other hand, it also changes the size of sonic line which traps the second mode acoustic waves, thus, altering the characteristics of second mode.

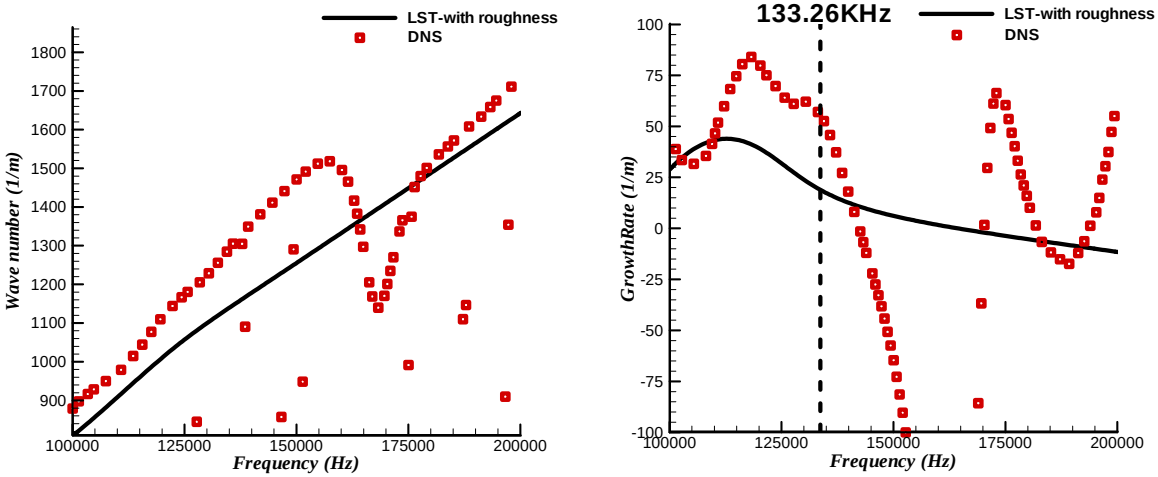

Figure 15. Comparison of LST prediction and DNS results on wave number and growth rate for meanflow with roughness $x = 0.17385m$.

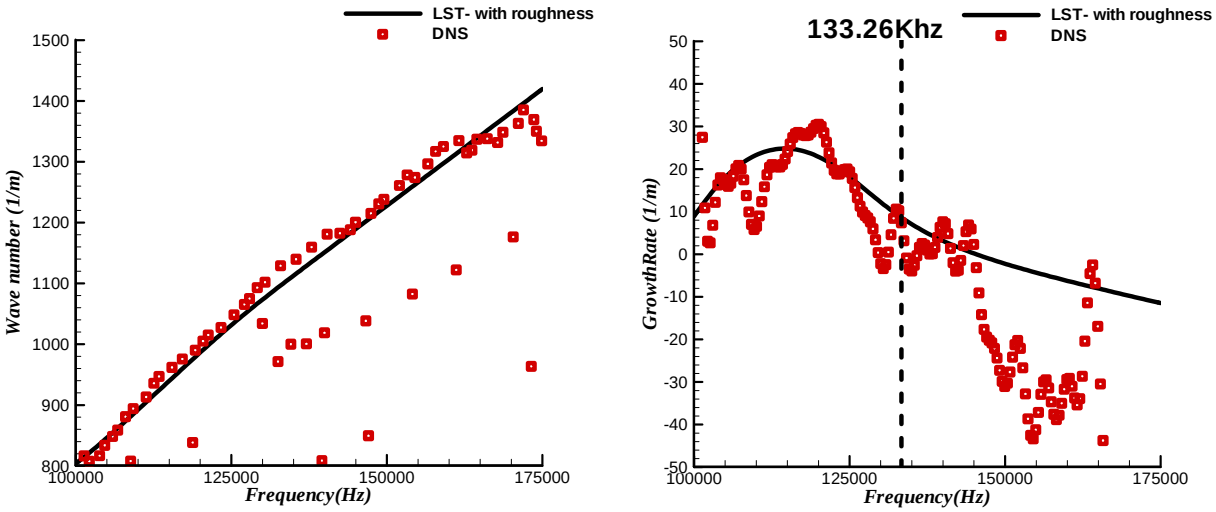

Figure 16. Comparison of LST prediction and DNS results on wave number and growth rate for meanflow with roughness $x = 0.26385m$

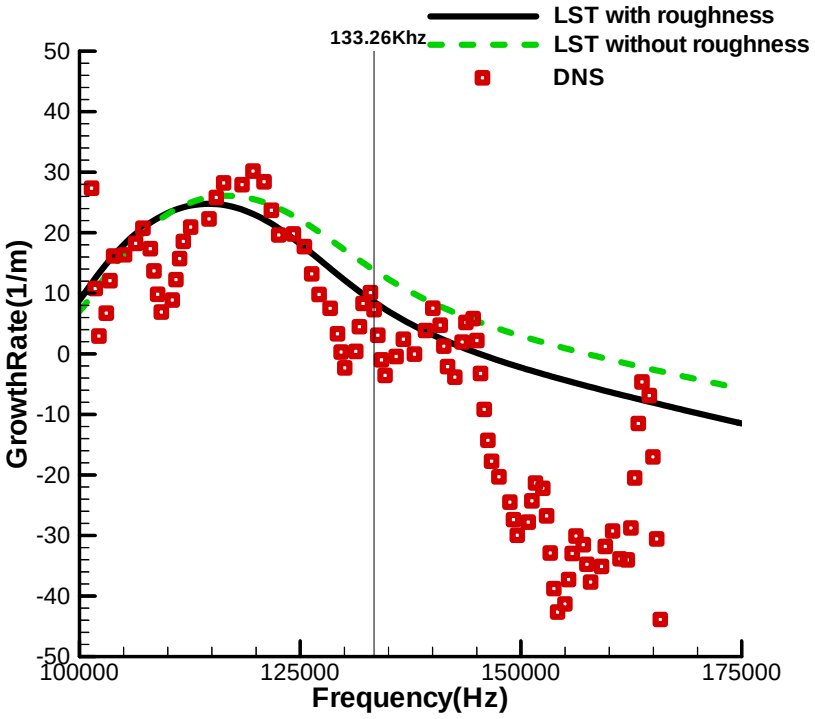

Figure 17. Comparison of LST prediction and DNS results on growth rate for meanflow with and without roughness $x = 0.26385m$

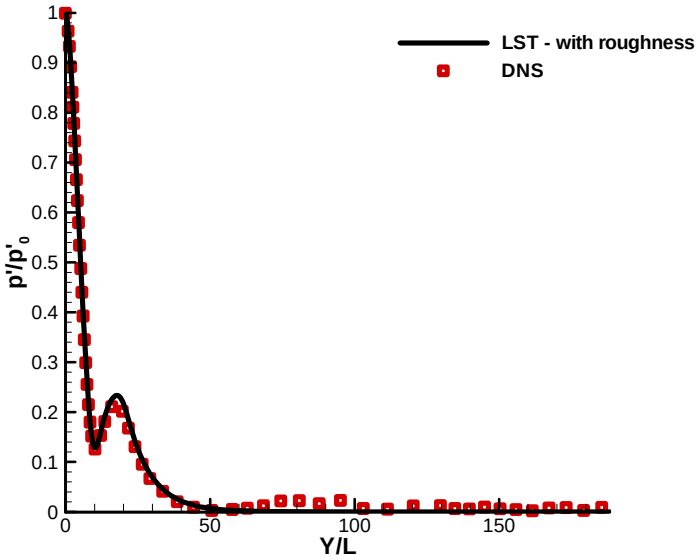

Figure 18. Pressure perturbation mode shape comparison at $x = 0.26385m$ for 118.9KHz

D. Supersonic Mach 3 Flow Simulation

Based on the simulation results, second mode is damped by roughness while first mode can be amplified. If the results are indeed valid, roughness element should amplify first mode pretention regardless of frequency. Therefore, a slower flow at Mach 3 flow in which second mode does not exist is conducted. The actual flow conditions are as following,

$$\begin{cases} P_r = 0.72, R_\infty = \rho_\infty u_\infty / \mu_\infty = 7.16\times10^6 / m \\ M_\infty = 3.0, T_\infty = 48.69K, P_\infty = 742.76Pa \end{cases}$$

It is widely known that second mode normally exists in a flow over Mach 4. As a result, the stability characteristic of a Mach 3 flow will be dominated by first mode only. Figure 19 (a) shows the phase velocities of boundary layer waves for the Mach 3 flow obtained by LST. It can be seen that Mode F and Mode S approach the sonic line asymptomatically and they never intersect, which implies no synchronization point exists in the flow. For comparison, the phase velocities plot for Mach 5.92 flow is shown in Figure 19 (b) in which clearly indicates the synchronization point where mode S and mode F cross.

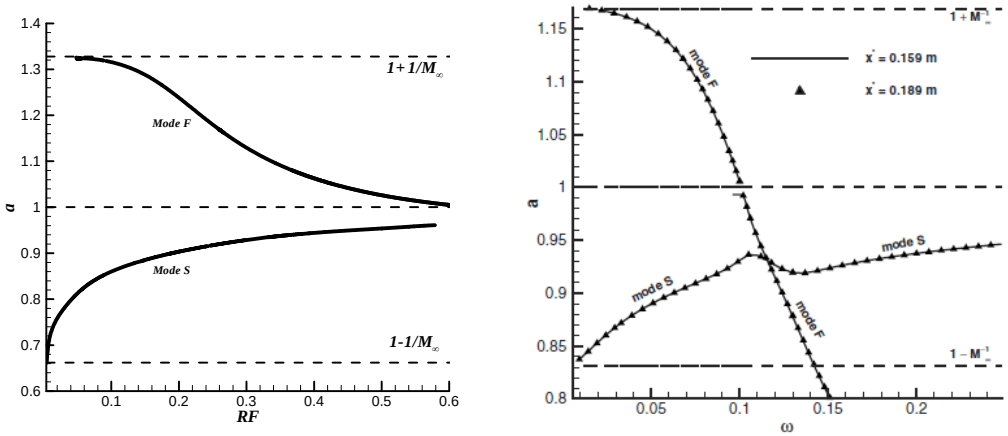

(a) **(b)**

Figure 19. Distributions of phase velocities of boundary-layer waves for (a) Mach 3 flow (b) Mach 5.92 flow

The pulse model which introduces a wall normal velocity pulse via a hole on a flat plate is implemented in the Mach 3 case for unsteady simulations. Figure 20(a) shows the wall normal velocity pulse has a Gaussian shape in time. An FFT analysis is performed on the velocity pulse. Figure 20(b) shows that the frequency range of the pulse is about $500Khz$, which is sufficient to cover the unsteady region of a Mach 3 flow. The hole is at $0.0416m$ from the leading edge of the flat plate with a width of $0.003m$. The location of roughness is the same as before at $x = 0.185m$. The main objective of this Mach 3 flow simulation is to confirm our hypothesis that roughness element is capable of amplifying first mode perturbation while it damps second mode perturbation. Since only first mode exists in this Mach 3 flow, roughness element on this flat plate should amplify perturbation of all frequencies. Figure 21 shows the numerical setup of the Mach 3 flow simulation. It can be seen that the wall velocity pulse has excited the boundary layer waves. The waves then propagate downstream and interact with the roughness downstream. Figure 22 shows the distribution of growth rate for modes F and S with respect to the dimensionless circular frequency. Figure 22 indicates that mode S is unstable from $\omega = RF = 0.009$ to 0.135. At the roughness location $x = 0.185m$, the unstable frequency range is from $3.74kHz$ to $56.08kHz$. To further validate the unstable modes in this flow are indeed first mode, the eigen-function or mode shape obtained from DNS is compared with the first-mode mode shape predicted by LST. Figure 23 shows the mode shape from DNS and LST at $38kHz$ and $x = 0.1811m$. This frequency is the most unstable mode in that location. It is seen that DNS and LST results agree very well, which suggests that the unstable modes in the flow are indeed the first mode.

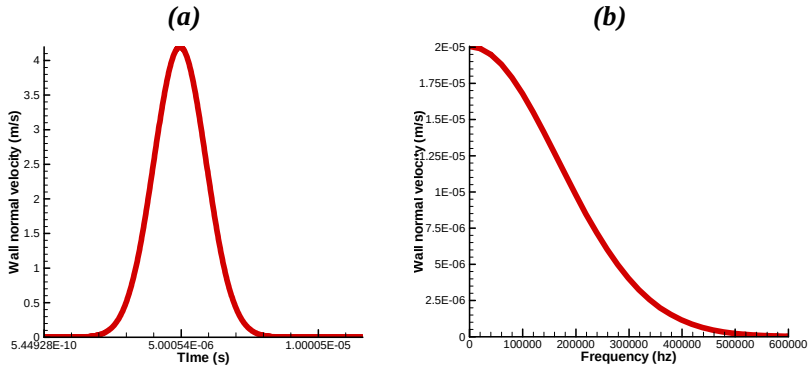

Figure 20. (a) Gaussian shape wall normal velocity pulse (b) FFT of the wall normal velocity pulse

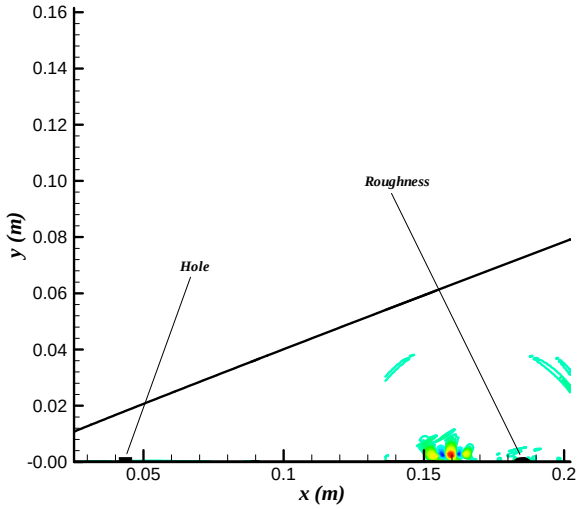

Figure 21. Schematic presentation of numerical setup for the Mach 3 pulse case

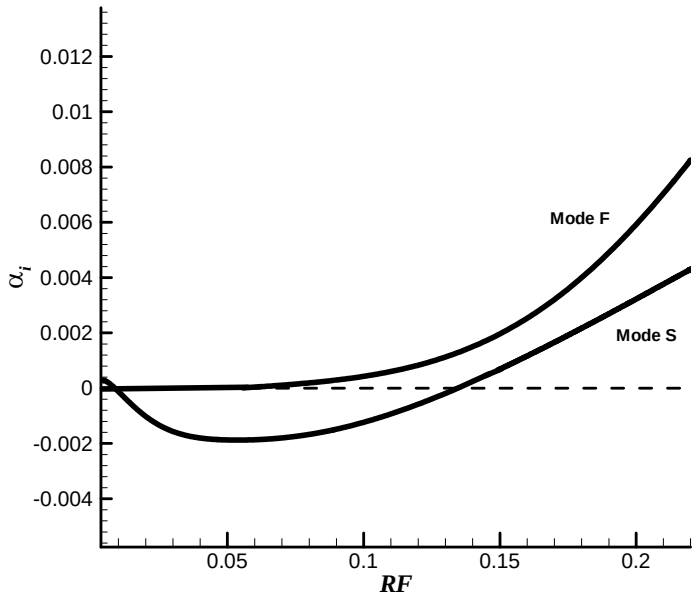

Figure 22. Distribution of growth rates of modes F and S

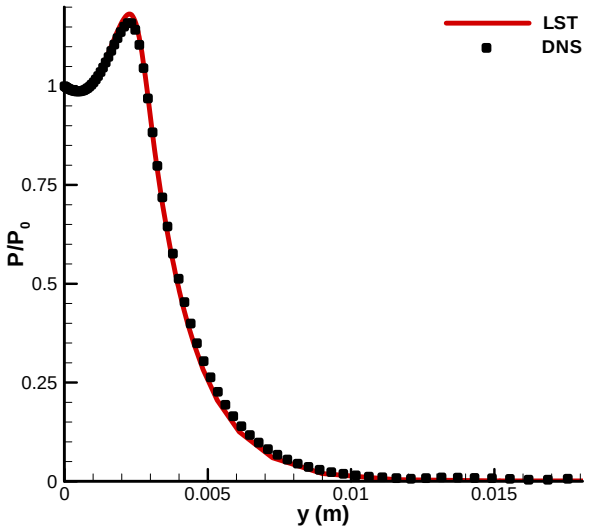

Figure 23. Eigenfunction/ mode shape at 0.1811m, 38kHz

As before, FFT analysis is performed to study the spatial growth of perturbation in streamwise direction. Figure 24(a) shows the frequency spectrum of different locations upstream of roughness. For comparison, the frequency spectrum of the same locations for no roughness case is shown in Figure 24(b). It can be seen that roughness amplifies perturbation for all frequencies. At $x = 0.13625m$, a location far upstream of roughness, the frequency spectrum of roughness and no roughness cases are very similar. However, as one moves downstream, at $x = 0.1511m$, roughness starts to have an amplifying effect on perturbation. At $x = 0.1811m$, a location very close to the roughness, the peak of the most unstable frequency is almost twice than the no roughness case. On contract,

for the Mach 5.92 simulation, roughness amplifies perturbations only at certain frequencies range, while it damps perturbation with frequencies higher than the synchronization point frequency as shown in Figure 4. Our previous conclusion about roughness and synchronization point has been validated in this test case.

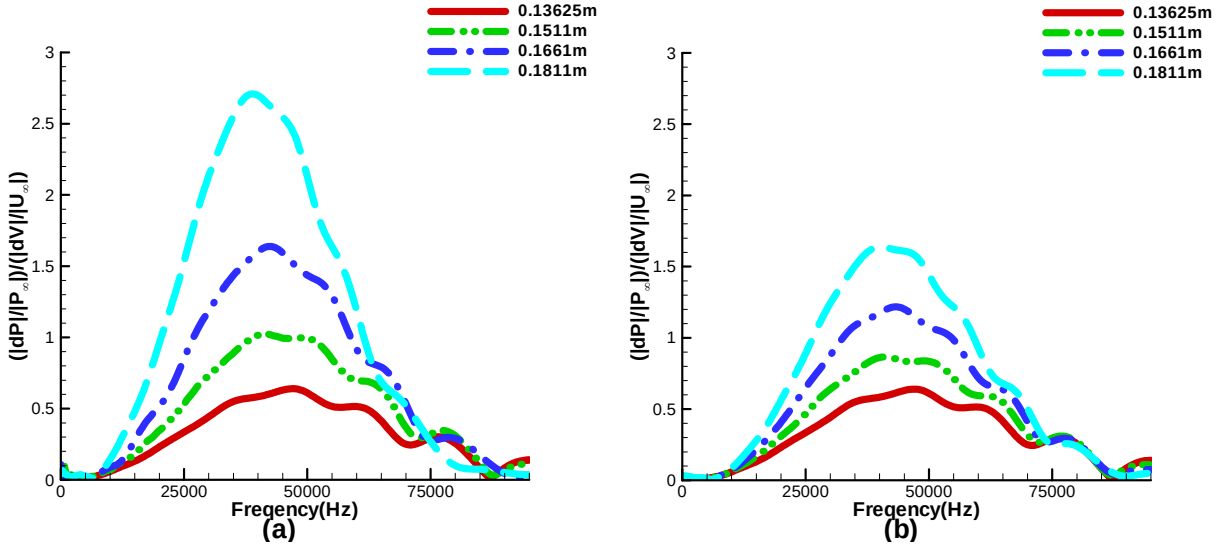

Figure 24. Frequency spectra for different locations upstream of roughness (a) roughness case (b) no roughness case

V. Summary and Conclusion

In the systematic studies, it has been shown that the relative location of roughness element and the synchronization point are important in determining the roughness effect on modal growth. Namely, roughness element is capable of amplifying perturbation at a frequency lower than the synchronization frequency (first mode perturbation), while it damps perturbations higher than the synchronization frequency (second mode perturbation). Previously, the systematic studies have considered different roughness locations/heights, different perturbation (Mode S/F), and perturbation at different frequencies. They are all pointing in the same conclusion.

In this paper, the systematic study is extended to include the effects of roughness width and multiple roughness elements. It is shown that the effect of roughness width is insignificant compared with the effect of roughness height as previously shown. Nevertheless, thin roughness results a stronger damping in the downstream region. In addition, it is shown that multiple roughness elements can be used to damp perturbations more effectively.

All new results are consistent with our primary observation about the synchronization point. Furthermore, the meanflow with and without roughness are examined trying to understand the mechanism of the damping and amplifying effects. It is found that a roughness element introduces infection points in the meanflow while it also alters the sonic line that corresponds to second mode instability.This alteration in meanflow can possibly be the reason of changes in the stability characteristics for mean flow with roughness. In addition, LST analysis is utilized to interpret roughness effect and show that it is able to predict the damping and amplifying effect that are observed in simulations. Given that LST is based on the meanflow profile, the agreement in LST strengthen the idea that changes of meanflow result changes in stability characteristics.

Since results show roughness element damps second mode only, a Mach 3 flow which only contains first mode is performed as a test case. LST shows that the synchronization location of this flow is infinite far from the leading edge. Therefore, any roughness element in this flow is located upstream of the synchronization point. Based on the hypothesis, a roughness element in this flow should amplify first mode for all frequencies. The results confirm this hypothesis and have indeed shown roughness amplifies perturbation at all frequencies. This further confirms the observations on the importance of the relative location of synchronization point and roughness elements by all of the numerical studies. The results can be a candidate to explain roughness delay transition as some experiments shown, and it also light up a new passive flow control method for hypersonic boundary-layer transition.

Acknowledgments

This work was sponsored by the AFOSR/NASA National Center for Hypersonic Research in Laminar-Turbulent Transition. Computer resources and supports are provided by XSEDE computing centers. The views and conclusions contained herein are those of the author and should not be interpreted as necessarily representing the official policies or endorsements either expressed or implied, of the Air Force Office of Scientific Research or the U.S. Government.

References

1. Schneider, S. P. "Summary of hypersonic boundary-layer transition experiments on blunt bodies with roughness, J. Spacecraft and Rockets," *Journal of Spacecraft and Rockets* Vol. 45, 2008, pp. 1090-1112.
2. Board, D. S. "Final report of the second defense science board task force on the national aero-space plane (NASP)." 1992, pp. 94-00052.
3. Anderson, J. D. *Hypersonic and high temperature gas dynamics*: AIAA, 2000.
4. Berry, S., Horvath, T. "Discrete roughness transition for hypersonic flight vehicles," *45th AIAA Aerospace Sciences Meeting and Exhibit*. Reno, Nevada, 2007.
5. Saric, W. S., Reed, H. L., and Kerschen, E. J. "Boundary-Layer Receptivity to Freestream Disturbances," *Annual Review of Fluid Mechanics* Vol. 34, 2002, pp. 291-319.
6. Mack, L. M. "Boundary layer linear stability theory," *AGARD Report*. 1984, pp. 1-81.
7. Maslov, A. A., Shiplyuk, A. N., Sidorenko, A., and Arnal, D. "Leading-edge Receptivity of a Hypersonic Boundary Layer on a Flat Plate," *Journal of Fluid Mechanics* Vol. 426, 2001, pp. 73-94.
8. Maslov, A. A., Mironov, S. G., Shiplyuuk, A. A., Sidorenko, A. A., Buntin, D. A., and Aniskin, V. M. "Hypersonic Flow Stability Experiments," Vol. AIAA 2002-0153, 2002.
9. Demetriades, A. "Hypersonic Viscous Flow Over A Slander Cone. Part III: Laminar Instability and Transition," *AIAA paper 74-535*, 1974.
10. Demetriades, A. "Laminar Boundary Layer Stability Measurements at Mach 7 Including Wall Temperature Effects," *AFOSR-TR-77-1311*, 1977.
11. Malik, M. R., Lin, R. S., and Sengupta, R. "Computation of Hypersonic Boundary-Layer Response to External Disturbances," *AIAA paper 1999-0411*, 1999.
12. Ma, Y., and Zhong, X. "Receptivity to Freestream Disturbances of Mach 8 Flow over A Sharp Wedge," *AIAA paper 2003-0788*, 2003.
13. Wang, X., Zhong, X., and Ma, Y. "Response of a hypersonic boundary layer to wall blowing - suction," *AIAA Journal* Vol. 49, No. 7, 2011, pp. 1336-1353.
14. Balakumar, P. "Transition In a Supersonic Boundary-Layer Due To Roughness Aand Acoustic Disturbances," *AIAA*. Vol. 3589, 2003.
15. Marxen, O., Iaccarino, G. "Numerical simulation of the effect of a roughness element on high-speed boundary-layer instability," *38th Fluid Dynamics Conference and Exhibit*. Seattle, Washington, 2008.
16. James, C. S. "Boundary Layer Transition on Hollow Cylinders in Supersonic Free Flight as Affected by Mach Number and A Screwthread Type of Surface Roughness," *NASA* Vol. memorandum 1-20-59A, 1959.
17. Holloway, P. F. a. S., J.R. "Effect of controlled surface roughness on boundary-layer transition and heat transfer at Mach numers of 4.8 and 6.0." Vol. TN-D-2054, NASA, 1964.
18. Fujii, K. "An Experiment of Two Dimensional Roughness Effect on Hypersonic Boundary-Layer Transition," *43rd AIAA Aerospace Sciences Meeting and Exhibit*. Vol. 2005-891, Reno, Nevada USA, 2005.
19. Fong, K., Wang, X. and Zhong, X. "Finite roughness effect on modal growth of a hypersonic boundary layer," *50th AIAA Aerospace Sciences Meeting Including the New Horizons Forum and Aerospace Exposition*. Vol. AIAA paper 2012-1086, Nashville, Tennessee, USA, 2012.
20. Fong, K., Wang, X. and Zhong, X. "Numerical Simulation of Roughness Effect on the Stability of a Hypersonic Boundary Layer," *Seventh International Conference on Computational Fluid Dynamics*. Vol. ICCFD7-2012-1502, Big Island, Hawaii, 2012.
21. Duan, L., Wang, X., and Zhong, X. . "A high-order cut-cell method for numerical simulation of hypersonic boundary-layer instability with surface roughness," *Journal of Computational Physics* Vol. 229, No. 19, 2010, pp. 7207-7237.
22. Whitehead, A. H. "Flow field and drag characteristics of several boundary-layer tripping elements in hypersonic flow," *Techinical paper, NASA* Vol. 5454, 1969.
23. Wang, X., and Zhong, X. "Effect of wall perturbations on the receptivity of a hypersonic boundary layer," *Physics of fluids* Vol. 21 No. 044101, 2009.
24. Fedorov, A. V. "Transition and Stability of High-Speed Boundary Layers," *Annu Rev Fluid Mech* Vol. 43, 2011, pp. 79-95.
25. Ma, Y. a. Z., X. "Receptivity of a supersonic boundary layer over a flat plate. Part 1. Wave structures and interactions," *Journal of Fluid Mechanics* Vol. 488, 2003, pp. 31-78.